Volume 4, Issue 1-4, 2017, 50 - 65 ISSN 2393-0586

Biomaterials and Tissue Engineering Bulletin

http://btebulletin.com/

Review Article Open Access Journal

Received: 10.04.2017 / Revised: 15.06.2017 / Accepted: 25.07.2017 / Published on-line: 11.08.2017

Nano-structured metal-semiconductor-metal photodetector for sensor network systems

Farzaneh Fadakar Masouleh[1, 2], Narottam Das[3, 4,*], Seyed Mohammad Rozati[1]

[1]Physics Department, University of Guilan, Rasht, Guilan 41938-33697, Iran;
[2]School of Engineering and Computer Science, Victoria University of Wellington, Wellington 6140, New Zealand;
[3]School of Mechanical and Electrical Engineering, University of Southern Queensland, Toowoomba, QLD 4350, Australia;
[4]Department of Electrical and Computer Engineering, Curtin University, Perth, WA 6845, Australia;

*corresponding author e-mail address: ***Narottam.Das@usq.edu.au***

ABSTRACT

The advanced and smart ways to produce complex nano-structures have incorporated new capabilities in various aspects of science and technology where structures on nano-meter scales are desirable including high-speed communication and sensor networks, and future biomedical sensors and detectors. In recent years, there has been a growing interest towards the miniaturization of optical and electrical components with faster and more efficient performance. The development of nano-materials and nano-structures design provides great opportunity for building multifunctional sensing elements which are smaller and more efficiently incorporated. Furthermore they have other useful characteristics like reduced production cost and minimized power consumption. Wireless sensor network systems have been identified as one of the most important technologies for the 21st century (Chong et. al., 2003). It can be deduced from its name that sensor network systems are composed of several sensor nodes, where each component is responsible for a function in the whole system, where it can consist of different kinds of sensors such as, thermal, visual, biomedical, infrared, acoustics, etc. Recent wireless communication system development requires a concurrent speedy advancement of sensors characteristics as well as the system performance. Therefore, it is very important to make the progress in sensors design with tiny dimensions, suitable for communication over a sensor network system with specified purposes such as, monitoring different parameters, namely humidity, temperature, light in household, cities, and different environments (Ian-Akyildiz *et al.*, 2002). The main focus of this review is to design and model an optimized plasmonics-based metal-semiconductor-metal photodetectors (MSM-PDs) with sub-wavelength architectures that is useful for high-speed optical communication systems and sensor network systems. Nano-structures designed on top of the electrodes trigger surface plasmon polaritons (SPPs) excitation and enable routing and manipulation of the light to be eventually trapped into the device active region.

Keywords: *MSM-PDs, Nano-structures, Subwavelength dimension, FDTD Simulations, Sensor Network Systems, Surface Plasmon Polaritons, Light trapping, Absorption enhancement***.**

1. INTRODUCTION

Photodetectors along with optical sources and fibers are most fundamental parts of all optical communication and related sensor network systems. The photocurrent (or voltage) is the output of a photodetector, also the detectable element by sensor network systems, computers, or other input terminals. There are broad range of properties, which are able to define the type of photodetectors. These requirements including detector's structure and active area, size, cost, sensitivity in specific frequency ranges, bandwidth, responsivity, and quantum efficiency provide various applications being used in sensor network systems, biomaterials imaging systems, etc. In previous decades, wireless network systems have been flourishing very quickly and among other concerns and requirements such as, spatial coverage, type, and security of the networks, the tendency towards the size modification and miniaturization of the sensor network systems has been growing significantly (Makki *et al.*, 2007; Noor *et al.*, 2012; Darrin *et al.*, 2004; Zimmermann *et al.*, 2004).

Photodetectors among basic optoelectronic devices are necessary for many applications in modern life. It is very important to design the detectors with improved ability to convert larger portion of the input light to photocurrent at the output. The photocurrents are the only input for all electronic devices such as, computers or other terminals at transmitting and receiving part of the communication systems (Pal, 1992). There are different types of photodetectors with various applications within electromagnetic (EM) spectrum. The photodetectors have fairly dynamic working ranges through the EM spectrum (such as, infrared, visible, and ultraviolet), so it has been designed for different applications. Also, some materials are more popular than others to build the sensors or sensor network devices. For example, internal photoelectric effect occurs in semiconductor while photoemission effect is mostly dominant in metals. Hence, in optical fiber communication systems, semiconductor photodetectors are preferred. These junction photodetectors have two operating modes either with zero bias as photovoltaic mode or reverse bias as photoconductive mode, having applications in solar cells and photodetectors, respectively (Agrawal, 2002). Solid state semiconductor photodetectors such as, positive-intrinsic-negative (pin) photodetectors, metal-semiconductor-metal photodetectors (MSM-PDs), avalanche photodiodes and heterojunction photodetectors are extensively used in optical wireless communication and sensor network systems. Photodetectors are one the more versatile technologies present in everyday life and have various applications not only in research but also in industry, and other entertainment systems. They are categorized according to their specific working ranges, i.e., the near-infrared region photodetectors, 0.8 to 1.6 μm, with high bandwidth and gain are very important as they have a wide variety of commercial and industrial applications in optical fiber communication and sensor network systems.

Among other photodetectors, the MSM-PDs have been extensively studied because of their remarkable high sensitivity-bandwidth product, ease of fabrication and ease of integration into monolithic receiver circuits, and wide range of useful applications in various areas. Hence, the MSM-PDs would be quite useful to provide miniaturized and optimized designs which collaborate in its better performance.

In the MSM-PD design, an undoped semiconductor is used as the substrate. In general, the photodiodes are composed of p-n junctions while in MSM-PD, there are two identical reverse biased Schottky diodes directly on the substrate. Interdigitated electrodes compose of alternatively biased closely spaced fingers. Our plasmonics-based MSM-PD with this electrodes design would have smaller carrier transit time, hence a higher bandwidth and a larger photo-absorption area for the detector providing an improved quantum efficiency (Chou *et al.*, 2002; Martín-Moreno *et al.*, 2001). Once the electrodes spacing is reduced to the diffraction limits, the active area becomes smaller and electrodes shadowing and reflectivity lowers the detector sensitivity. The MSM-PDs utilize very low dark current because the current flow is blocked from the metal to semiconductor due to the existence of two Schottky barriers. A pin photodetector consists of an intrinsic region usually an undoped semiconductor sandwiched between the n-type and p- type semiconductors, and it is known to have a low capacitance. However, MSM-PDs with equal light sensitive area compared to pin photodetectors have much lower capacitance which stems from their geometry and design utilizing interdigitated electrodes. Shining the light through photodetectors active region or applying an electric field or a voltage across the detector's electrodes originates the electrons and holes. Then, a photocurrent is created due to electrons and holes drift towards opposite electrodes. Hence, the light absorption in the subwavelength slit region of the device boosts due to the recombination of electron and hole pairs (Ozbay., 2006).

High-speed photodetection presents an interesting new design for pioneering telecommunication and wireless sensor network systems. A transmission medium or waveguide such as, an optical fiber cable provides a channel for the signal to propagate with minimal losses, and receivers like pin photodiodes or photodetectors form the principal parts of modern optical telecommunication systems. Usually, a laser or a light-emitting diode (LED) provides the source to an optical network, by converting the electrical input into light waves. One of the major part of a receiver is the photodetector and its key role is to generate electrical signals from optical input signals. To have fast, broad bandwidth, reliable and cheaper optical communications and interconnect systems, high-performance optical receivers as a basic part should meet the requirements and keep up with the fast growing technology. Wide bandwidth and low capacitance MSM-PDs show dominantly higher performance and are extensively used in optical receiver. Most of the modern integrated optoelectronic circuits are tightly coupled with new generation of high sensitivity MSM-PDs. Furthermore, compared to the conventional photodetectors, the MSM-PDs have faster response time, as well as much lower noises and dark current. Hence, the next-generation optoelectronic technology needs alternative optimized systems like MSM-PDs for applications in high speed optical communication and signal processing, also super-fast chip-to-chip optical interconnects.

In the past, the micrometer-scale bulky components of photonics limited the integration of these components into electronic chips (White at al., 2006), however this problem has been prevented by implementation of surface plasmon-based (SP-based) circuits which merge electronics and photonics utilizing nano-meter scale components. Designing constant pitch nano-gratings on optical devices bring an advantage of efficient light transmission, absorption or confinement with aid of surface plasmons (SPs) (Yu *et al.*, 2006; Grote *et al.*, 2010; Krenn *et al.*, 2001; Park, 2014), and this is where a new branch of photonics, called plasmonics, was introduced which is simply the optics of metallic nano-structures (Sambles *et al.*, 1991; Lindquist *et al.*, 2012). The new plasmonic technology improved MSM-PD's performance significantly. Nano-structures are used to improve light capturing capacity in a plasmonic-based MSM-PD via surface plasmon resonances. Hence, because of the small spacing between the Au contact fingers, detector's response time is low, while its responsivity has improved significantly (Karar *et al.*, 2013; Karar *et al.*, 2011).

In modeling, generally Gallium Arsenide (GaAs) semiconductor is used as the substrate. The GaAs is preferred for the design of electronic and photonic devices because of its unique electrical and optical properties as a compound semiconductor (Cha, 2004). The GaAs substrate provides wide range of bandwidth and good responsivity characteristics due to GaAs's short absorption length. Being a direct bandgap semiconductor, it can collect and emit light more efficiently than indirect band gap semiconductors. The GaAs has a conduction-band structure that leads to fast electron conduction. Furthermore, it is suitable for infrared range applications because of its wide bandgap.

Depending on the gratings application, they are designed to be responsive to one or more diffraction orders. For zero order gratings, the grating pitch is smaller with respect to the illumination wavelength, hence, other than zero order, higher orders of diffractions are not involved (Raether, 1988; Mawet *et al.*, 2006; Kikuta *et al.*, 2003; Kikuta *et al.*, 2003). In situation where the grating pitch is much smaller than the wavelength, the structures are called subwavelength nano-gratings. As a result, there is no diffraction in a subwavelength grating, and the grating area can be assumed to have homogeneous optical properties according to the effective medium theory (Schmid *et al.*, 2008).

For gratings with sizes smaller than the incident light wavelength, the interacting light becomes resonant, then it reflects throughout the slits and a series of resonant reflection occurs. Due to the rapid development of advanced nano-based research and its potential applications in photonic devices and technology, it is important to fully understand the dielectric response of metals.

Photonic components and integrating photonic devices are increasingly achieving more functionality and playing a vital role in making progress in novel technological trends.

For this instance, the photonic insulating properties of metals can be used to trap an incident light concentrating in very small areas (Lezec *et al.*, 2002). Not many years ago, energy localization and enhanced optical properties of metal nano-structures and thin films under electromagnetic wave illumination has been discovered (Dhakal, 2009; Battula *et al.*, 2007). Among optical nano-structures, unlike what is believed by the standard aperture theory, subwavelength slits has been proved to have exceptional properties in which light can be transmitted higher order of magnitude due to the contribution of SPPs in extraordinary optical transmission (EOT) (Das *et al.*, 2011; Wijesinghe *et al.*, 2011; Martín-Moreno *et al.*, 2003; Das *et al.*, 2009, Das *et al.*, 2010).

In recent years, there has been an increasing interest focusing on the design and characterization of novel types of nano-photonic devices (Bozhevolnyi *et al.*, 2005; Lee *et al.*, 2007; Kim *et al.*, 2008). Concentrating the light into small areas with the aid of extremely thin layers of negative dielectric constant under electrostatic condition creates a plasmonic lens. A series of interactions in the nano-scale leads to EOT occurrence which is a unique phenomenon due to involvement of nano-scale periodic patterns, slits, or holes and excitation of SPPs with light illumination. While EOT basics contradict the diffraction limit as a conventional optical constraint, it is believed that evanescent modes are enhanced through interaction with subwavelength apertures/slits. This procedure includes the multiple diffraction of light as a result of the captured light matching with periodic nano-gratings to provide SPP wavevectors, followed by the wavevectors moving over the nano-structures, reaching the nano-sized aperture, and providing resonance enhancement through the slit in the substrate at the near-field of the device. Many metallic nano-sized structures including subwavelength slits have plasmonic effects and can form a high light concentrated region with respect to the light wavelength and the geometry of nanostructures.

With the development of plasmonic-based research approaches to improve the field interactions efficiently inside the metallic nano-structures, a meaningful relation has been reported for the EOT in subwavelength plasmonic gratings. However, the EOT mechanism is not yet fully understood and is under investigation for further improvement. As we know metals are opaque and very reflective. The frequencies within visible spectrum are all absorbed inside the bonds and can move through the metal by electron transition because of their empty electron states. When illuminated on the surface, metals reflect almost all the energy with the same incident wavelength as the absorbed light is re-emitted by the surrounding free electrons and that is why the metal surface is glossy or shiny. Among these, noble metals have fabulous properties which enable them to contribute in a diverse range of plasmonic applications. For plasmonic interactions to occur, some metals with special characteristics are required. As a result, the interaction of light with resonant nano-structures at the interface between metal and dielectric creates the SPPs. Actually the metal plays a more important role than dielectric in plasmonic applications and that is because of their unique electrical and optical properties involving the large number of free electrons. Starting from visible wavelengths, plasmonic applications have found their way through different parts of the electromagnetic spectrum. The important notice is the form of metals that are used in plasmonic, which is the nano-structured metals and not the bulk form. The most famous example in ancient glass industry is the roman Lycurgus Cup from the 4th century (Atwater, 2007). This cup turns color when illuminated from inside and outside. This effect is attributed to fabulous plasmonic resonances in visible wavelength and it was suggested that the silver and gold nanoparticles are responsible for the green and red colors produced by the cup, respectively.

Interest towards plasmonics grew after observation of anomalies in optical reflection by Wood on metallic nano-gratings, which was later explained by Rayleigh's diffraction theory. Since the nano-structured noble metals satisfy the free-electron theory, the SPs excitation can easily occur within plasma frequency. The EOT enhancement for nano-structures is an interesting property which is conjugated with plasmonic related field localization. The EOT and its high energy concentration effect have potential applications in novel photonic and optoelectronic systems, and near-field microscopy.

It is considered a key challenge to keep up with the rapid nano-science progress and understand how tailoring the elements up to nanoscale dimensions affect many areas of research. This fact provides wide range of interesting applications and opportunities that can only be achieved by understanding fundamentals for design, and optimization of subwavelength dimension structures. Miniaturization of optical and electrical components provides faster and more efficient functionalities which are not predictable at large scale. These devices majorly contributed in development of high-speed telecommunication systems and sensor networks, integrated biosensors, computers capacity and storage properties, solar cells, photodetectors, etc.

The growing interest toward plasmonics combined with exploitation of new properties in nanotechnology research incorporated new capabilities in various aspects of science and engineering that reinforced the possibilities for design and fabrication of nanoscale systems including metallic nano-structures. Manipulating commercial plasmonics-enhanced MSM-PDs as part of these development essentially relies on SPPs ability to confine electromagnetic energy flow in nano-scale dimensions.

As mentioned, SPPs excitation is among one of the absorption anomalies plasmonic nano-structures can easily exhibit. In the presence of a transverse magnetic (TM) polarized light, the SPs exist along a metal-dielectric interface. According to the device characteristics and application, periodic one-dimensional (1-D) (which applies to our design), or two-dimensional (2-D) metallic nano-gratings can be helpful to couple the illuminated light with surface evanescent excitations and transmit the propagating SPPs through the central slit. Surface excitations decay perpendicularly along the structure. The excited SPPs as horizontal surface resonances can be moved to the central slit through periodic nano-gratings while they acquire propagating feature perpendicular to the grating grooves. Fundamental modes created in central slit can be associated with Fabry-Perot vertical cavity resonances. The energy flux reaching the subwavelength slit, consecutively reflects from top and bottom. Hence, the enhanced transmission through the semiconductor substrate is caused by the fundamental TM guided modes in the slits, being affected by both nano-gratings geometry and Fabry-Perot resonances (Collin *et al.*, 2002; Ceglia *et al.*, 2010). Furthermore, both horizontal and vertical surface resonances contribute to EOT occurrence (Porto *et al.*, 1999).

Nowadays, the effect of material selection to produce EOT is known, as this quality has a close relation with further development of nano-plasmonic devices. The frequency dependent electric permittivity (i.e., dielectric constant) of noble metals describes their electromagnetic energy characterization and optical properties which has a complex form like εm=ε′m+iε″m. It consists of a real part ε′m with negative value and an imaginary part ε″m with positive value. The bigger imaginary part has the greater absorption loss. Here, the material dispersion characteristics including electric permittivity values are calculated from Lorentz-Drude model. The notation i is an imaginary unit for complex numbers, and εd is the electric permittivity of the surrounding medium, in our case it is air.

2. SURFACE PLASMON RESONANCE IN PRISM AND DIFFRACTION GRATINGS

The SPs are quantas of plasma existing at the interface of the metal and dielectric. These surface electromagnetic waves decay exponentially with respect to the interface. At metal-dielectric interface, the excitation of SPs is not spontaneous and a coupling mechanism is required. The first method to trigger surface plasmon resonances is using a prism, either Kretschmann or Otto configuration. These two prism configurations are very similar and their only difference is in the middle air gap between the metal and prism, which exists in Otto configuration but not in Kretschmann. The prism configuration works when the total internal reflection (TIR) condition is satisfied. In this method, plasmons are coupled to the evanescent wave, and surface plasmon polaritons are created. They can enhanced transmission and reduce the reflection losses. At a specific angle, called resonance angle, the reflection reaches to its minimum.

Nowadays, nano-gratings have become very popular in optics and related studies participating in many cutting-edge researches. There are some kinds of nano-gratings with different behaviors such as, diffraction, reflection, transmission, and phase of nano-grating. Each nano-grating structure is composed of ordered corrugations on a substrate which will interact with a frequency comparable to its dimensions. The nano-gratings can be either called continuous or discontinuous regarding the materials used to build the nano-grating and the substrate.

Subwavelength nano-gratings have found remarkable applications in nanotechnology. Being illuminated with a p-polarized electromagnetic wave, a diffraction nano-grating provides different orders of diffraction denoted as d as shown in equation (2). The orders would be some integer numbers both positive and negative, with zero being the order without any diffraction. The light interacts with the subwavelength gratings and passes through the corrugations. The number of diffraction orders available after the gratings are in direct relation to the period of the grating and the incident light wavelength. Zero-order gratings are the kinds which only produce the zero order, d=0, which means any diffraction is banned and the behavior of the device should be studied according to the laws of reflection and refraction.

The light bends as it passes through small slits/ apertures or towards the edges and corners of an object. This causes diffraction, if the light is interacting with a feature comparable to the wavelength of illumination. This fact is described by Huygens-Fresnel principle, i.e., each point on the wavefront is perceived as a source point, and the traveling wavefronts generate new wavefronts propagating in every direction. The wavefront may have coincidence with another wavefront, then wave interference will occur. Hence, a diffraction pattern is produced.

Under a monochromatic light illumination, each slit acts as a light source diffracting the light into discrete directions which depends on the light wavelength. Diffraction gratings can be reflective or transmissive, but the most important property of these gratings, which is creation of diffraction orders, is observable in both of them. Single ray diffraction on a plane surface results in a single transmitted and single reflected rays, while the advantageous of using periodic perturbations on the surface is to create various diffraction orders which usually provides additional information about the light interaction after the gratings. Application of metallic nano-structures in the second way excites plasmon resonances. However, any metal piece cannot be used for plasmonic applications. The condition for the existence of the SP on a flat air-metal interface, $\varepsilon'_m<-1$, $\varepsilon''_m<<|\varepsilon'_m|$, is fulfilled for some metals, e.g., noble metals, including the silver (Ag) and gold (Au) (Masouleh *et al.*, 2013; Sturman *et al.*, 2008; Zhang *et al.*, 2007). Also, according to the electrostatic limit in which the metal nano-structures should be smaller than the wavelength in dimension, only the non-magnetic properties of these metals are preserved.

3. BASICS OF THE FDTD SIMULATION METHOD

Finite-difference time domain (FDTD) method is a powerful simulation tool to solve the partial differential equations numerically (Jin, 2010). The FDTD simulation method is simple and it utilizes the central difference approximation to discretize the two Maxwell's curl equations, namely, Faraday's and Ampere's laws, both in time and spatial domains, and then it solves the resulting equations numerically to derive the electric and magnetic field distributions at each time step using an explicit leapfrog scheme. The FDTD solution, thus derived, is second-order accurate, and is stable if the time step satisfies the Courant condition. One of the most important attributes of the FDTD algorithm is that it is appropriately parallel in nature, i.e., parallel processing in both the time and spatial domains, because it only requires exchange of information at the interfaces of the sub-domains in the parallel processing scheme, which consequently makes it faster and more efficient to obtain the simulation results (Yu, 2009).

4. THE YEE ALGORITHM

The FDTD algorithm was originally proposed by K. S. Yee in 1966 (Yee, 1966) that introduced a modeling technique with second order central differences to solve the Maxwell equations applying finite difference approach (or mathematics). One of the advantageous of FDTD algorithm is its ability to simply calculate the values of electromagnetic field components like E (Electric field) and H (magnetic field) on edges of the meshing network directly at specific points of space with defined x, y, and z. Many optimized versions of the primary algorithm have been developed during the years which make it compatible with applications in almost every electrical and photonic systems.

5. TM WAVES FOR FDTD SIMULATION

In 2-D FDTD simulation for the TM wave (Ex, Hy, Ez - nonzero components, propagation along with Z, transverse field variations along with X) in lossless media, Maxwell's equations use the following form:

$$\frac{\partial H_y}{\partial t}=\frac{1}{\mu_0}\left(\frac{\partial E_x}{\partial z}-\frac{\partial E_z}{\partial x}\right),\ \frac{\partial E_x}{\partial t}=\frac{1}{\mu_0}\frac{\partial H_y}{\partial z},\ \frac{\partial E_z}{\partial t}=\frac{1}{\varepsilon}\frac{\partial H_y}{\partial x} \qquad (1)$$

The location of the TM fields in the computational domain (mesh) follows the same philosophy as shown in the following Figure 1.

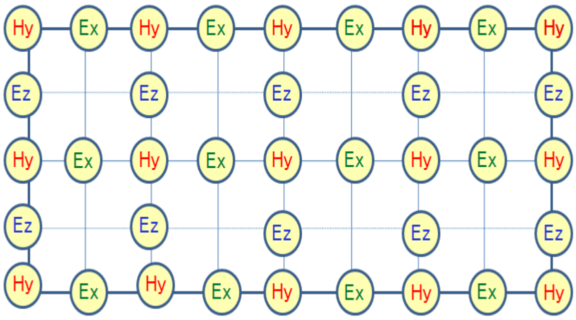

Figure 1. Location of the TM fields in the computational domain of FDTD algorithm.

In this case, the electric field components Ex and Ez are associated with the cell edges, while the magnetic field Hy is located at the center of the cell.

For extraordinary light transmission to occur not all materials are suitable. Ideal materials to trigger the EOT are noble metals like Ag, and Au arranged in periodic patterns or holes, which is mainly due to their plasmonic properties. At the interface between two materials (usually dielectric-metal interface) with opposite signs in electric permittivity, the conditions are satisfied for the SPs to exist. The real part of complex dielectric constant on metal side should be negative, while the absolute value of the imaginary part is small. This is not fulfilled for many metals, even for well-known plasmoinc materials like silver and gold plasmonic properties changes through the EM spectrum. If the dielectric constant is complex then the kspp is also complex. According to the SP dispersion relation, SPPs are generated only on the right side of the light cone. The real kspp is always bigger in value than the outer line of the EM light cone wave vector (kspp>k0), this fact makes the SPPs to be non-radiative and decay at the interface. Hence to generate SPP modes, a coupling mechanism is surely needed.

6. MODELLING CONDITIONS OF NANO-STRUCTURED MSM-PDs

Optiwave FDTD (Opti-FDTD) is one of the most commonly used methods, highly integrated, and user-friendly software that allows computer aided design and simulation of advanced passive photonic components. It allows modelling and analysis of sub-micron or subwavelength designs with accuracy. The Opti-FDTD software package is based on the FDTD method. The FDTD method has been established as a powerful engineering tool for design of integrated and diffractive optical devices. This is due to its unique combination of features such as, the ability to model light propagation, scattering and diffraction, and reflection and polarization effects. It can also model material anisotropy and dispersion without any pre-assumption of field behavior such as, the slowly varying amplitude approximation. A sub-micron or nano-scale feature implies a high degree of light confinement and correspondingly, the large refractive index difference of the materials (mostly semiconductors) to be used in a typical device design (Finite Difference Time Domain Photonics Simulation Software, version 8).

We have conducted a 2-D FDTD study from Opti-FDTD module, a software package developed by Optiwave Inc. The Opti-FDTD is one of the most practical simulation tools that fully satisfies our study requirements to analyze the performance of plasmon assisted MSM-PD. This method translates the physical structure into a mathematical model and a numerical procedure via differential equations. The design model is basically divided into small grids to form square lattice called mesh along the structure's cross-section. The mesh step size (Δx) is considered to be around 10 nm with a time step size being Δt < 0.1 Δx/c all over the computational domain. Here, we don't present simulations with mesh grid size of less than 10 nm, because of computer memory issues (e.g., computer capacity), and the fact that it is extremely time consuming, while the simulations results for even 2 nm meshing size is almost identical to 10 nm. We designed the device inside an anisotropic perfectly matched layer boundary condition (APML) along both x- and z- axis. The APML is a very efficient FDTD boundary conditions and has an accredited theory, its outside boundary is assumed to be reflecting a portion of the power into the primary computational zone so a boundary truncation occurs for perfectly conducting wall. The implementation of the APML boundary conditions complies with a Maxwell-based formulation rather than a mathematical model, for this reason the APMLs are recognized as physical rather than numerical boundary conditions (huping *et al.*, 2008).

In our modelling with FDTD method, the incident light normally hits the surface of the nano-gratings, interacts with it and is driven through the central slit and finally improves the absorption inside the semiconductor. Because of GaAs's electrical and optical properties, it is an excellent candidate for many optoelectronic and photonics applications preferred over other semiconductor materials. So that the detector presents high multiple responsivity-bandwidth product. Upon illumination from top, the surface plasmon interactions in metallic nano-structures and consequently the light absorption is enhanced near the semiconductor interface, hence the free electron-hole pairs are generated. The nano-gratings on top of the electrodes create a plasmonic lens, and these nano-structures are essential for light confinement through the subwavelength volumes. They squeeze the light in nano-meter dimensions, and have the ability to trigger SPP-generated localized regions of the high-intensity electric field which is an essential requirement for EOT through the MSM-PD central slit.

Lorentz-Drude model presents an accurate and convenient technique to describe the dispersion properties of materials. Dielectric properties of nano-structures in our simulation are determined with this model. The semiconductor substrate is made of GaAs, which provides useful properties such as, low dark current in electrical properties aspect, and high-efficiency light emission in optical properties aspect, and application in optoelectronic devices e.g., GaAs MSM-PDs, and GaAs solar cells (Tan *et al.*, 2010; Das et al, 2012). Gold (Au) has well-defined plasmonic characteristics and low dissipation in the near-infrared spectral region. We designed devices with inter-digitated electrodes and the nano-gratings on top of the electrodes using gold (Sturman *et al.*, 2008). Therefore, to reduce the reflections losses from the edges of the 2-D FDTD computation lattice, a powerful absorbing boundary condition is applied both on the horizontal and vertical sides. The polarized illumination light in z-direction was selected to be a Gaussian-modulated continuous wave with the central wavelength of 830 nm in the corresponding pulse. Light polarization affects the SPP excitation. To trigger plasmon excitation and satisfy the wave vector matching at the metal surface with any mechanism, e.g., prism or nano-gratings, TM polarization is suitable, which is because of its electric field including a vertical component. TE polarization has a parallel electric field component, hence unable to excite surface plasmon modes.

In Figure 2, we presented the schematic view of our 2-D simulation design for plasmonics-based MSM-PD. This high performance device is composed of a semiconductor substrate responsible for collecting the energy. Here, the central slit region which enhances and leads the energy flux to the substrate, and the nano-gratings region which plays a very important role in coupling the incident illumination are shown. The slit width parameter should lie within a certain interval to efficiently enhance light absorption inside the active region of the photodetector. This parameter should be small enough to trigger plasmonics and Fabry-Perot enhancement, and reasonable dimensions to be fabricated. Among several simulated models, 50 nm slit width has shown good light capturing capacity that directly affects the device performance. A wider slit width, e.g., 100 nm presents promising results and because of its larger dimension, compared with thinner slits e.g., 50 nm or smaller, also has the benefit to be easily fabricated. MSM-PDs is a nano-scale device that has an excellent quality to achieve better light absorption compared with a similar sized pin photodetectors, by which we mean their active area. That is resulted from special type of combined electrodes in MSM-PD that provides a very small gap between two electrode types, hence, reduces the dark current and increases the bandwidth.

Furthermore, improved field interaction in the near-field is associated with interaction of evanescent modes created in vicinity of periodic nano-structures and subwavelength slits area which is the main light source for SPP interactions. Hence, an accurate design for metallic nano-gratings including proper pitches and shape for nano-structures provides promising condition for SPP excitation.

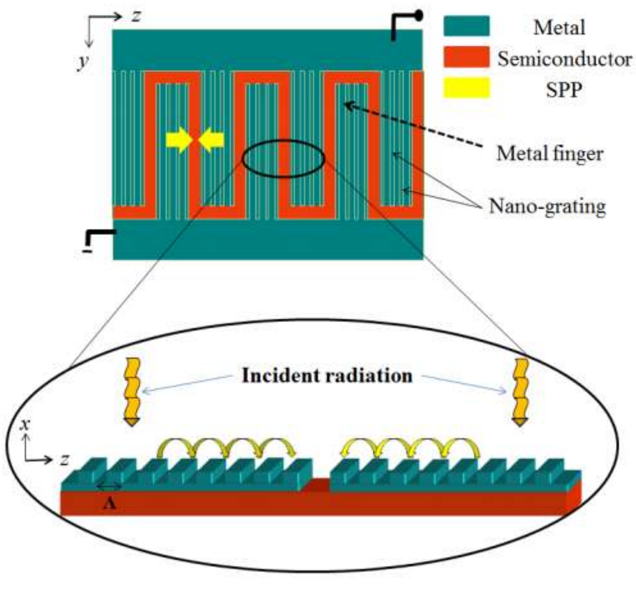

Figure 2. The top view of MSM-PD with rectangular shaped nano-gratings and its interaction at the central slit are shown. The subwavelength slit is just on top of the semiconductor substrates.

Mainly originating from surface plasmon excitations, an energy confinement is generated in a single subwavelength slit which leads to enhanced light transmission under certain circumstances. This can be considered as spectacular advances in light flow and interaction which creates opportunities for advancement of a variety of optical devices with different materials working through wide range of wavelengths (Hibbins *et al.*, 2004; Akarca-Biyikli *et al.*, 2004; Beruete *et al.*, 2004). In the subwavelength slits, depending on the geometry and size, the properties of the Fabry-Perot cavity resonances occur and the light continuously re-emits back and forth in the main slit of the photodetector. In our plasmonic-based MSM-PD, transmission absorption process in the subwavelength slits is partly driven by Fabry-Perot resonances. Particularly, the SPPs which result from incident light wave vector matching with the nano-features, are concentrated by the active region of the device and are potentially suitable for growing field of nano-scale optics and photonic circuits. Furthermore, excitation of symmetric SPP modes cause partly or fully resonance absorption of incident light during interaction.

Our periodic nano-gratings are continuous as they are designed on top of metallic contacts both made of Gold. Interaction of surface electron densities and the electromagnetic waves generates the SPPs which by nature have decaying behavior, however, they can efficiently trap the excited high energy waves in the device active region. On the surface of materials with large amount of free electrons e.g., metals, collective interactions occur which allows light concentration in subwavelength volumes, below the diffraction limit of light. Compared to light, SP has longer wave vector in the dispersion curve, and is not radiative by nature.

To excite SPs however there should be some periodic nano-grating features with scrutinized dimensions with respect to the incident light wavelength to satisfy coupling conditions. The SPP wave vector matching condition with the famous grating equation at metal-dielectric interface which provides a relationship between the nano-grating period, light wavelength and different orders of diffraction, is a modified version of the prism resonance equation (Bera *et al.*, 2012). Hence, the SPPs propagating constant or wave vector can be written as follows (Raether, 1988; Shackleford *et al.*, 2009):

$$k_{spp} = \frac{\omega}{c}\sin(\theta) \pm \frac{2\pi d}{\Lambda} = \frac{\omega}{c}\sqrt{\frac{\varepsilon'_m \varepsilon_d}{\varepsilon'_m + \varepsilon_d}} \qquad (2)$$

In equation 2, Λ is the periodic nano-gratings' pitch, ω inserts the incident light wavelength impression in terms of the angular frequency, c denotes the speed of light in air, θ is the defined incidence angle with respect to the surface normal, and d is an integer number, i.e., d = 1, 2, 3, …, N.

At a typical frequency, the light wave vector is always smaller compared with the SPP wave vector. Designing a nano-grating structure provides an extra momentum to match the SP wave vector, therefore the light wave vector is coupled to SPPs wave vector. At the metal-dielectric interface, the electric permittivity changes sign if the host material is suitable to trigger SPPs. As mentioned earlier, metal permittivity is complex and varies with wavelength, considering eq. 2, the SP wave vector is complex. The imaginary part of the wave vector parallel component is responsible for decaying nature of the SPP while propagating at the interface. To overcome the damping behavior of the plasmonic material in the specified working wavelength, we choose the gold material that has relatively a large negative real part which satisfied the energy confinement condition, and very small imaginary part which is responsible for the losses. The left side of equation (2) under proper field interaction, becomes equal to the k vector of excited SPP, kspp.

The constraint in our modelling was to constantly satisfy the symmetric arrangement of nano-gratings, that is setting the number of pitches equal on both sides with respect to the central slit. With aim of developing the nano-grating assisted MSM-PDs performance, and based on the peculiar interest in studying the behavior of new generation of nano-structures, we investigated the performance of geometrically different plasmonics-based MSM-PD designs. For a set of 1-D nano-gratings, the corrugations length is infinite, in our case in the y-direction. Here, in the modified nano-grating assisted structures, depending on the identical materials used to build the thin layer under the nano-gratings, the rectangular nano-gratings structure can be called as continuous.

7. LORENTZ-DRUDE MODEL

Well-established Lorentz-Drude model found its way through simulation tools for characterizing optical and electrical components. Optiwave provides the opportunity to efficiently use Lorentz-Drude model while doing simulation with FDTD method. Multi-pole dispersion model is used for gold, and the Lorentz-Drude model is written for 6 resonant frequencies (LD6). The resonant frequency changes with the oscillating strength. We can utilize Lorentz-Drude model in both frequency- and time- domain with the specific related conditions.

7.1. Lorentz-Drude Model in Frequency Domain.

Combining Lorentz model and Drude model leads to a more versatile model which can easily describe dielectric and magnetic properties of metals closer to the experimentally measured functions for a wider range of EM spectrum while each model separately fails in some specific ranges. Famous metal conductors like silver, and gold have complex dielectric functions below plasma frequency, hence, it is useful to present a refined model like Lorentz-Drude which fits the material properties. The complex dielectric function for a group of materials, which sums up both intraband, εrf(ω), and interband, εrb(ω), effects, is denoted as follows (Rakic *et al.*, 1998):

$$\varepsilon_r(\omega) = \varepsilon^f(\omega) + \varepsilon^b(\omega), \qquad (3)$$

In equation 3, the dielectric function for metals according to Lorentz-Drude model is shown as εr(ω). The free electron effects or Drude model is stated by εf(ω). It is quite efficient for predicting the transport properties of electrons in metal conductors in conjunction with optical properties of material. εb(ω) or Lorentz model is a semi-quantum model for dispersive media describing bound electron effects. Each of Drude model and Lorentz model is suitable for different frequency ranges and materials, which means that dielectric function values reported for each of them would be different from the other model. Equations (4) and (5) display the mathematical formula for Drude and Lorentz model, respectively (Markovic *et al.*, 1990).

$$\varepsilon^f(\omega) = 1 + \frac{\Omega_p^2}{j\omega\Gamma_0 - \omega^2}, \qquad (4)$$

$$\varepsilon^b(\omega) = \left(\sum \frac{\Omega_p^2}{\omega_m^2 - \omega^2 + j\omega\Gamma_m} \right), \qquad (5)$$

In (4) and (5), the plasma frequency is denoted as Ωp=G01/2ωp, in which G0 is the oscillator strength. Γ0 is the damping constant. Each oscillator is defined with a number (m) and has the angular frequency of ωm and lifetime of 1/Γm. The combined equation representing the Lorentz-Drude model satisfying complex index of refraction for materials like Ag and Au is written as:

$$\varepsilon_r(\omega) = \varepsilon_{r,\infty} + \sum_{m=0}^{M} \frac{G_m \Omega_p^2}{\omega_m^2 - \omega^2 + j\omega\Gamma_m}, \qquad (6)$$

For infinite frequencies εr,∞ is the relative permittivity. Gm specifies the strength of mth resonance term, ωm is the angular frequency of the mth resonant mode, and Γm is the damping factor.

7.2. Lorentz-Drude Model in Time Domain.

The Lorentz-Drude model shown in (6) is in the frequency domain form. However, the FDTD is a time domain method and therefore it would be suitable for broadband simulations. Therefore, we need to convert (6) to the time domain form, so that the FDTD can handle the full wave-analysis for the Lorentz-Drude material. This transformation to time domain is accomplished by using the Polarization philosophy within Maxwell's equation as given below. The Lorentz-Drude model in time domain can be expressed as follows (Finite Difference Time Domain Photonics Simulation Software):

$$\mu_0 \frac{\partial \vec{H}}{\partial t} = \nabla \times \vec{E}, \qquad (7)$$

$$\varepsilon_{r,\infty}\varepsilon_0 \frac{\partial \vec{E}}{\partial t} + \sum_{m=0}^{M} \frac{\partial \vec{P}_m}{\partial t} = -\nabla \times \vec{H}, \qquad (8)$$

$$\frac{\partial^2 \vec{P}_m}{\partial t^2} + \Gamma_m \frac{\partial \vec{P}_m}{\partial t} + \omega_m^2 \vec{P}_m = \varepsilon_0 G_m \Omega_m^2 \vec{E}, \qquad (9)$$

Thus the FDTD algorithm is derived based on the above equations. Nowadays, the FDTD method is very much efficient, accurate and widely used for electromagnetism computations such as, fields and resonant modes. The FDTD software based simulation results have demonstrated significant enhancement of light absorption for the design of ultrafast MSM-PDs (Tan *et al.*, 2010; Sharma *et al.*, 2002, Dahawan *et al.*; 2011, Yoon *et al.*, 2006).

8. SIMULATION RESULTS AND DISCUSSION

We present different types of nano-grating design and simulation results of plasmonics-based MSM-PDs. Application of the subwavelength plasmonic nano-structured gratings enables the MSM-PD to interact strongly with the incident light as they are able to influence the SPPs coupling and propagation. The SPPs generate localized region of high intensity electric field and can improve the light absorption efficiency into the active region of the semiconductor substrates, GaAs. Hence, the coupling process which directly contributes to the quality light confinement in the active region of the photodetectors is significantly affected by the proper size limitation and the nano-gratings optimization. This energy concentration strongly depends on the geometrical parameters, i.e., shape, number, width, and height of the nano-gratings. Furthermore, we will examine the effect of thin film application inside the central slit that is greatly involved with the device efficiency in light harvesting and confinement.

A practical method to measure the amount of light energy guided to the MSM-PDs active region is to introduce a representative which compares the amount of light transmitted through the plasmonic device with the conventional MSM-PD which does not have plasmonic effects. This parameter is named as light absorption enhancement factor (LAEF). In next section, we used the term LAEF. LAEF is a useful dimensionless value, to compare different MSM-PDs performance with each other.

8.1. Electrodes Surface Coverage with Nano-gratings.

In this section, we discussed if changing the number of nano-grating on each side of the slit will affect the absorption quality of the device. This would be an advantageous result for experimental purposes as limiting gold usage reduces the fabrication expenses. For this analysis, while keeping the device symmetric, the number of nano-gratings on each side of the slit is increased starting from one. The grating pitch is kept constant at 810 nm which is a bit lower than the illumination wavelength, hence preserves the plasmonic conditions. The subwavelength slit width is selected as 100 nm. The underlayer thickness should also be thin enough to satisfy plasmonic conditions, therefore it is designed as 60 nm thick. In this simulation procedure, the nano-gratings height which is mostly responsible for surface plasmon excitations is considered to be 100 nm. Figure 3 displays the resulted maximum LAEF for MSM-PD structures considering different number of nano-gratings symmetrically designed on the sides of the central slit. The transmission curves show that with the increase in the numbers of nano-gratings, N, the LAEF enhances and it saturates when the value of N is 4 or higher.

As can be seen, starting from a specific value, increasing the number of nano-gratings will not affect the amount of transmitted light into the device's active region. It can clearly be explained by SPP characteristics which is in close relation with the nano-structures geometry and the incident light wavelength. As SPPs must have a wavelength shorter than the illumination light, they definitely have to decay in a distance shorter than nano-grating period, which has a size around the light wavelength. Another reason would be the reduction of SPP resonance's amplitude while passing through the nano-gratings area combined with the enhancement in the propagating length of the plasmonic resonances and re-radiation of SPP waves as they propagate through the remnant part of the design through the central slit.

There would always be some part of light energy which reflects back from the nano-grating structures to the air. Hence, the amount of this light energy losses, we measure the light reflection factor from the structure in the subwavelength region. Figure 4 illustrates the calculated amount of reflection loss factor for a plasmonics-based MSM-PD. The interesting result is that a peak in absorption occurs when the reflection is minimum. The reflection curves behavior is similar to the absorption curve. This means that, while the reflection spectrum gives identical results for the number of nano-gratings more than 4, between 1 ~ 3 the light reflection spectrum increases for each higher value of N.

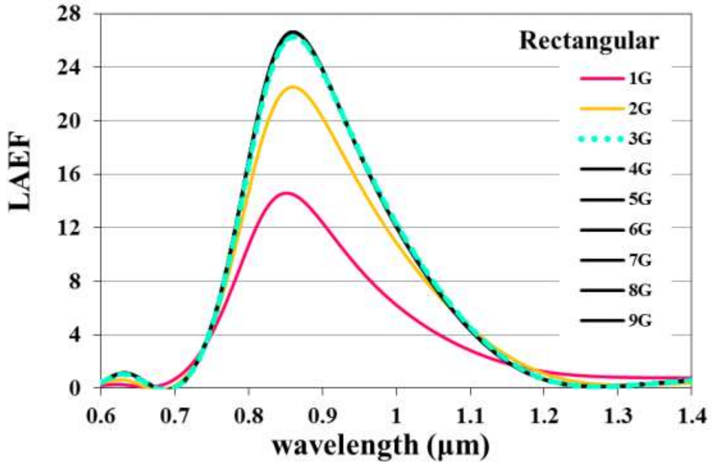

Figure 3. LAEF curves for different number of nano-gratings symmetrically arranged on both sides of the slit for plasmonic-based MSM-PD structure. As it can observed that the absorption curves for N>4 are completely overlapped.

We also indicated how the incident angle affects the maximum LAEF for several designs with different number of nano-gratings responsible for plasmonics interaction, however the symmetric condition should be satisfied for the device.

Several simulation curves have been produced, each one having different angle of incident. The incidence angle variation is in the range of -90° ~ +90°, with respect to the normal axis on the surface. The negative angle is measured from the normal to the left and positive angle shows the angle opening from the right side. The most efficient illuminating angle which indicates the maximum LAEF is shown in Figure 5.

Also, according to the presented results, the incident angle behavior for different numbers of nano-gratings are in agreement with previous simulations in Figure 3. As shown the resonant angle is about -46° for this typical geometry with the value of 947 nm for resonant wavelength.

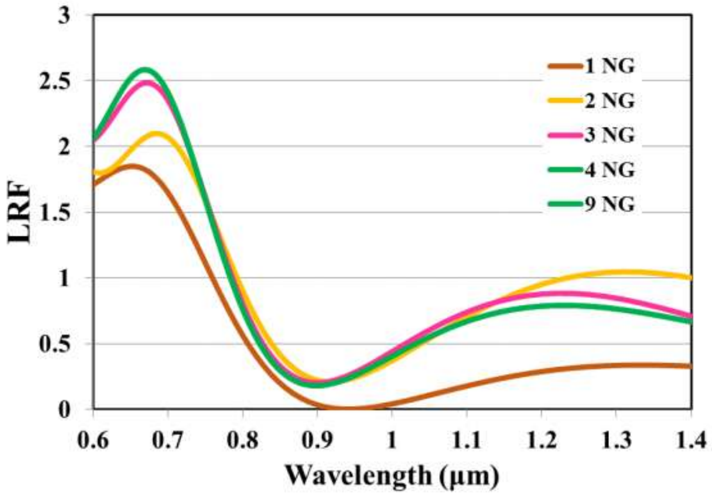

Figure 4. Light reflection factor (LRF) curves for different number of nano-gratings (1 ~ 9) symmetrically arranged on both sides of the slit for a plasmonic-based MSM-PD structure.

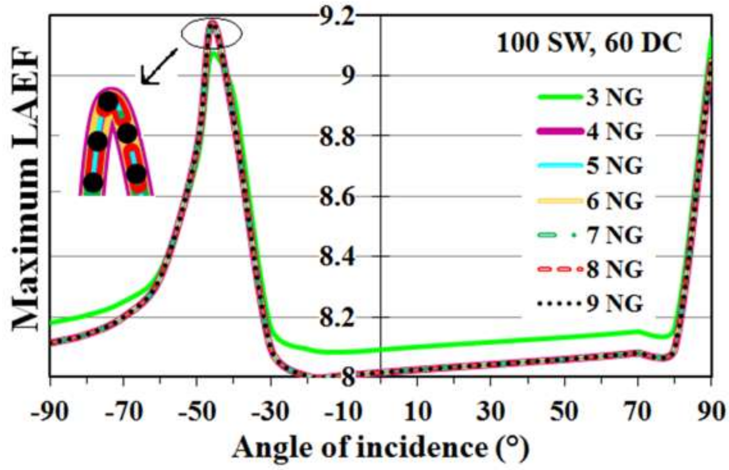

Figure 5. Effect of the incidence angle variation on light absorption curves. Maximum values for each LAEF curve is selected to produce the LAEF curves versus incidence angle for plasmonic-based MSM-PDs. The simulations were performed for different number of nano-gratings on each side of the slit [Das *et al.*, 2014].

Other than investigating the number of nano-gratings that cover the electrode surface, it is quite useful to study the duty cycle (DC) of corrugation effect on LAEF, which is also a parameter changing the device absorption capability directly influenced by the surface coverage with nano-gratings. Duty cycle gives a ratio for the percentage of ridges width to the nano-grating period, i.e., 60% DC refers to one nano-grating period in which the ridge ratio to the whole period is 3 to 5.

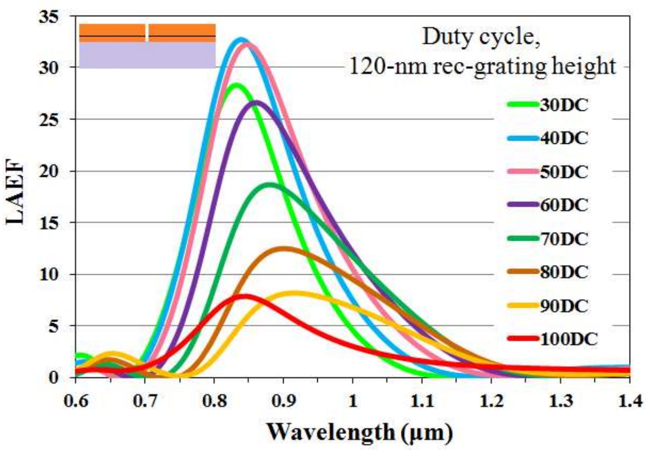

Figure 6. LAEF spectra for 10% to 100% DCs in MSM-PD with rectangular-shaped nano-gratings. Here, the nano-gratings height is 120-nm and subwavelength slit width is 50-nm. Inset shows the cross-section of rectangular-shaped nano-gratings when the DC is 100%.

In this modelling, the subwavelength slit width, the underlayer thickness, and the nano-gratings height has been kept constant at 50 nm, 20 nm, and 120 nm, respectively. Figure 6 shows how the DC can affect the energy flux behavior inside the active region of the MSM-PDs as well as the peak wavelength at the maximum LAEF point. It can be inferred that optimal plasmonics focusing cannot be achieved for all DCs as the peak wavelength and the maximum LAEF changes for each curve. As can be seen, the maximum LAEF occurs for 40% DC for this specific design with the value of ~33. The curve for 100% DC is the case in which a plasmonics MSM-PD is changed to conventional MSM-PD because with full DC the nano-gratings are not existing any more, as shown in inset of Figure. 6, the device is a conventional MSM-PD with the underlayer thickness of about 140-nm which is the sum of nano-gratings height with full DC and the underlayer thickness.

8.2. Ellipse-wall Plasmonics-based MSM-PD.

The nano-structures on metallic surfaces provide an interesting plasmonic application to increase the light confinement inside the active region of the device, which is useful for optical instruments, photodetectors, and photovoltaic devices (Das *et al.*, 2011; Ko *et al.*, 2011). Surface plasmons created on the metal-dielectric interface are evanescent with decaying characteristics, it means that if they are not enhanced by the nano-gratings, the corresponding energy will be lost. Hence, optimization of the MSM-PD performance is a lot dependent on the nano-gratings geometry. The rectangular-shaped nano-gratings has been suggested to be the primary design for nano-gratings, probably because of their simple features and reasonable plasmonic performance. Using a specific equation for design of an efficient nano-grating shape, e.g., ellipse-wall (EW) nano-gratings result in an increased light absorption process. The exponential function of z = Aex with A=3 being the exponential coefficient provides the best design for EW nano-gratings curvatures. Figure 7 shows the absorption curves for different EW nano-grating heights, having a peak for 140 nm. Furthermore, the forth absorption curve in Figure 7 indicates the absorption behavior for rectangular nano-grating assisted MSM-PD at its optimized height, that is 140 nm, while DC is 40% and central slit width is 50 nm for all designs.
Therefore, we conclude that replacing sharp edges with non-linear walled features is advantageous for our MSM-PD, i.e., carefully designed curvature facilitates plasmon interactions and energy flow through the plasmonic device active region. Therefore, the LAEF is improved ~17% compared to a rectangular-shaped nano-grating MSM-PD.

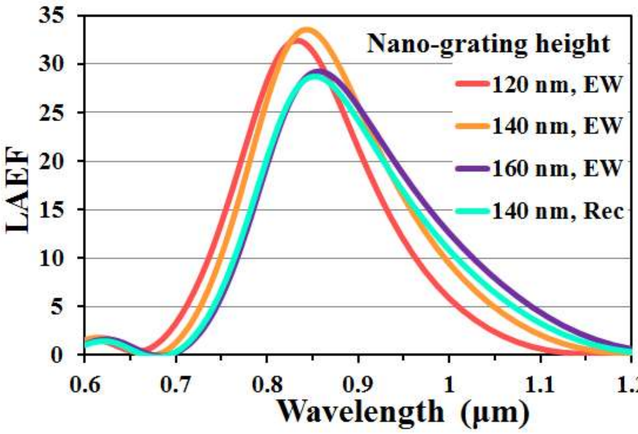

Figure 7. LAEF spectra for ellipse-wall (EW) and rectangular (Rec) plasmon-assisted MSM-PDs with different nano-grating heights. There is about 5 unit difference between Max LAEF for 140 nm height REC and EW nano-gratings design .

8.3. Effect of metallic electrodes Thickness.

Metallic electrodes are one of the conventional and most essential parts of MSM-PDs. As mentioned before, in order to increase the photodetector's absorption efficiency, the metallic nano-gratings are applied on top of the electrodes which work as active layer in the photodetector. However, optimization of active layer or underlayer thickness (Uth) affects the LAEF in the MSM-PD. The active layer thickness is an important variable for development of the MSM-PD. A big part of the illumination is absorbed in thick active layer, hence better carrier recombination effect but reduced quantum efficiency. While improved optical properties, higher carrier collection and modified electrical properties is provided for thin active layer apart from material saving to build thinner layer (Shen *et al.*, 2009). In both cases adding plasmon coupling element improves the detector's absorption quality.

Underlayer thickness is an important parameter for improving plasmonic applications. For optical-plasmonic applications producing thin layers of metals is of great importance for optical energy transmission and excitation. In our MSM-PD design, we are interested in increasing the absorption factor, hence we can reduce the electrodes thickness which contain the central slit in the middle, so that the plasmonic interactions are strengthen in the nano-grating grooves in addition to the central slit and can be transmitted through the thin metal electrodes.

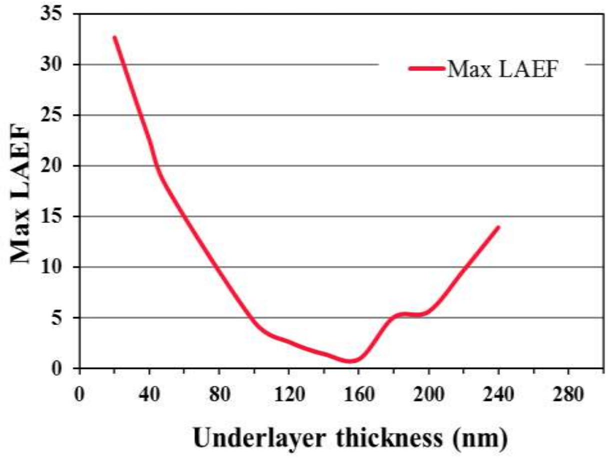

Figure 8. The maximum LAEF points for various underlayer thickness with steps of 20-nm are shown. The thinner underlayer thicknesses have the best performance.

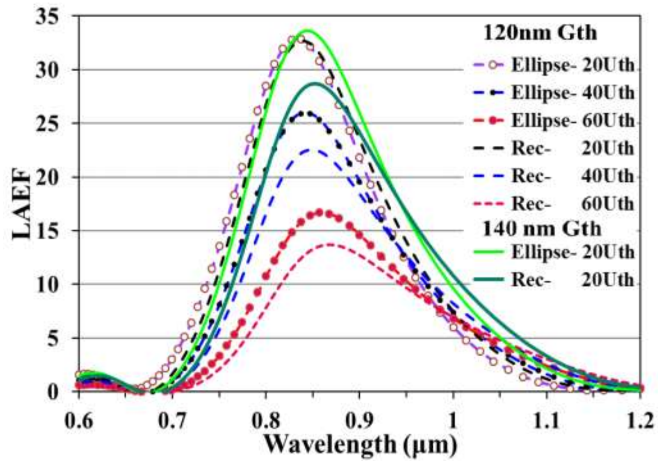

Figure 9. Comparison of LAEF for MSM-PDs with three different underlayer thicknesses (Uth). The LAEF curves for rectangular and ellipse-wall nano-gratings with optimized nano-grating thicknesses (Gth).

We changed the underlayer thickness for a rectangular-shaped nano-grating assisted optimized MSM-PD with the nano-grating thickness of 120 nm. Specified maximum points in LAEF curve shown in Figure 8 confirms that before reaching the first minimum in sinusoidal curve that is around 160 nm underlayer thickness, the LAEF increases rapidly as the active layer height decreases. This means that decreasing the subwavelength aperture thickness assists the light intensity to couple more efficiently/effectively from the nano-gratings to the subwavelength aperture region.

The curvature dependent LAEF for two inverted ellipse-wall nano-gratings with convex and concave structures are shown in Figure 10(b) which is directly proportional to different exponential coefficients of -5 and +5 for two geometries, respectively. For the case of underlayer thickness as 20 nm, structures with exponential coefficient of -5 with convex walls have the maximum LAEF among other inverted ellipse-wall structures. Moreover, for inverted ellipse-wall structures with exponential coefficient of +5, the performance becomes weaker however the absorption yet depends on the underlayer thickness. Also, the inverted structures are not convenient for nano-grating design as they are less stable and show weak absorption results.

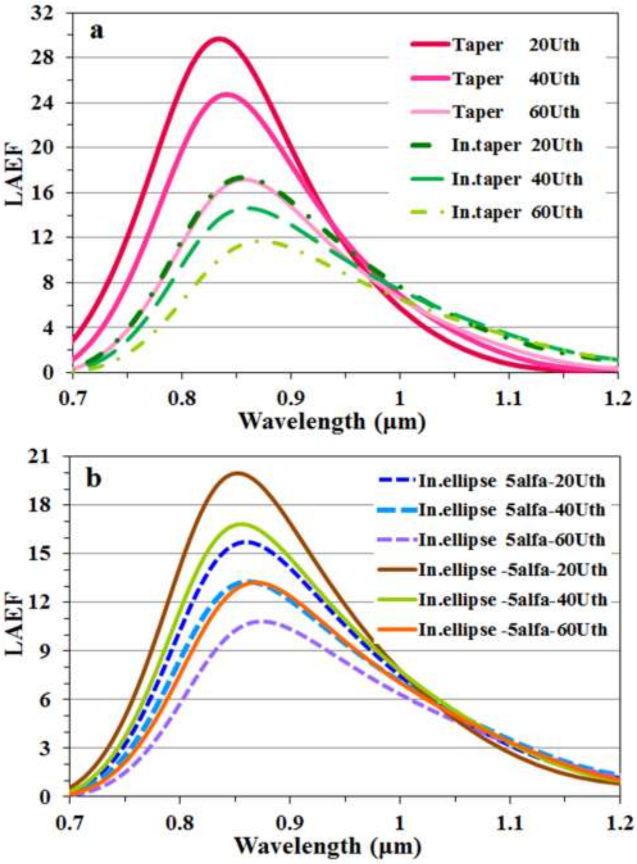

Figure 10. Comparison of LAEF for MSM-PDs with three different underlayer thicknesses (Uth): (a) with trapezoidal (Taper) and inverted trapezoidal (In.taper) profiles and (b) with inverted ellipse-wall nano-grating profiles (In.ellipse) and exponential coefficients of +5 and −5. The structures have 0.9 AR for all simulations.

8.4. Ultra-thin Metallic Film Assisted MSM-PD.

In this section we discussed the goal to determine the influence of a thin metallic slab inside the central slit flanked by metal nano-gratings and confirmed that it has boosted the energy localization in the photodetector's active region. This happened due to the interaction of the photons and the potential free electrons presented in the metallic thin film. Hence, the most efficient design for energy concentration leads to a strong light absorption through the subwavelength slit and inside the substrate. Based on the simulation results, we confirmed the improved performance of MSM-PD with application of thin layer of Au symmetrically inside the central slit. Optimization of this design boosts the light absorption and focus in addition to the nano-gratings application for plasmonic MSM-PD.

Fast decaying evanescent modes in metallic components through coupling with light and interacting with nano-grating wave vector are enhanced and lead effectively to the semiconductor substrate after resonances enhancement through Fabry-Perot excitations inside slit because the thin metallic slab in the central sub-wavelength slit of the plasmonics-based MSM-PD works as a planar waveguide. Hence, the plasmonic lens with its negative permittivity in the frequency range of interest provides the characteristics for creation of a perfect focal point at near-field in which both propagating and evanescent waves contribute. Combination of EW nano-gratings plasmonic effect and optical concentration of ultra-thin film enhances plasmonics-based MSM-PD's performance.

The EM energy existing inside the slit includes both propagating and evanescent waves. The evanescent waves decay exponentially, however they contain very fine information in subwavelength scale. Nano-structured negative index media (NIM) presents fascinating prospects for light manipulation (Zalevsky *et al.*, 2010). In 2000, Pendry (Pendry *et al.*, 2000) suggested that a slab of NIM can be a 'perfect lens' (Shalaev, 2007), in which the evanescent waves are enhanced through the slab instead of decaying while propagation. This offers the possibility of restoring or recovering the lost information.

The key feature of a negative index metallic slab is to enhance the evanescent waves resulting in a sharper image. This quality has beaten the diffraction limit and led to useful improvements in near and far-field microscopy (Veselago, 1968, Liu *et al.*, 2007). Hence, sharper image utilizing very fine structural details are obtained in microscopy (Zhang *et al.*, 2008). In addition to this exciting property being applied to improve imaging techniques, we can use the optical concentration ability of nano-structured NIM to enhance the light absorption performance of the proposed plasmonic MSM-PD.

We replaced or deformed the existing central slit geometry and applied a nano-sized ultra-thin film inside it and designed the nano-gratings to be ellipse-walled for further absorption improvement. The results indicate that by changing the size features of the ultra-thin film, the transmission properties inside the substrate can be tuned correspondingly.

EW nano-gratings are new kind of nano-structures, the cross-section is shown in Figure 11, to be placed on the metallic contacts with non-linear walls. The simulation results indicate that for the MSM-PD, these alternative geometries are well suited to be replaced with traditional kinds of nano-grating geometries, e.g., rectangular. The EW nano-grating design provides light transmission efficiency over rectangular-shaped (Rec) nano-gratings. Because of the broader slit opening, there would be a low amount of reflection loss, and the light capturing process would be more efficient and focal energy areas at the sharp edges will be avoided because of the special design for the central slit opening which is no sharp angle on the entrance of the slit. Apart from their special design which allows more energy flux involved with the SPP interactions inside the slit, we decided to do modelling on EW nano-gratings because of their identical shape with experimental nano-grating SEM or AFM images.

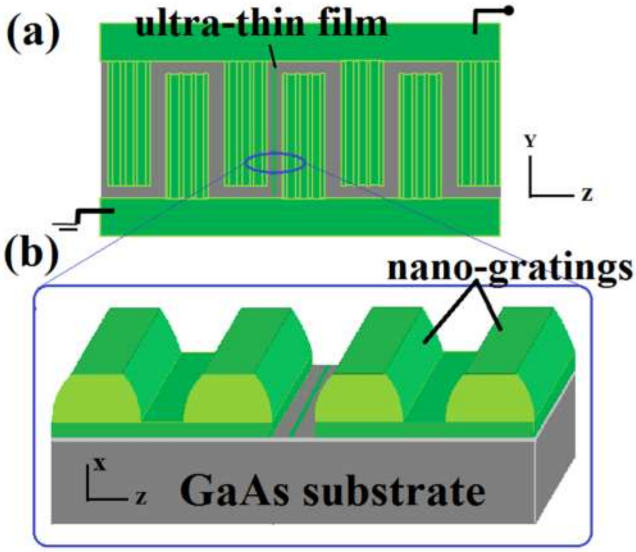

Figure 11. . Schematic design of top view with a magnified side view for plasmonic-based MSM-PD. Nano-gratings are ellipse-walled shape and they are placed on metal contacts. The ultra-thin film is inside the subwavelength slit. (a) Top view of MSM-PD, (b) Magnified cross section of MSM-PD

Finally, the light capturing efficiency for two symmetrically designed plasmonic-based MSM-PDs, with and without ultra-thin film assisted central slit, were calculated.

The absorption improvement in the MSM-PDs is caused mostly by plasmonic effects that includes wave vector mixing and energy enhancement by nano-gratings which is eventually lead through central slit. Also, the Fabry-Perot resonances in the nano-grating grooves and most effectively in the central slit. Our suggested design also utilizes the improving effects of ultra-thin metallic film inside the subwavelength slit through SPP characteristics. Hence, to satisfy plasmon resonance condition and Fabry-Perot amplifying effects, it is crucial to properly design central slit's dimension to be well beyond the incident light wavelength to satisfy subwavelength design's conditions.

It is clear that the application of the ultra-thin film provides plasmonic effects and assists in concentration of light in the active region.

However, optimizing the nano-gratings height is another straightforward modification which has a similar effect towards improving the device efficiency. Different ultra-thin film assisted devices absorption curves with nano-grating heights varying around the previously attained optimized EW nano-gratings height are shown in Figure 12(a) which indicates significant light absorption enhancement for the new symmetric design due to improved SPP excitations, with the peak of absorption at 140 nm for the nano-grating height.

While all three heights present more suitable results compared to their bare slit plasmonic-based counterparts, the peak wavelength is red shifted. Furthermore, we are interested to see if this resonant absorption caused by the nano-scale feature in the slit is affected by its geometry.

Hence we designed several MSM-PDs each time covering different portion of the active layer surface (central slit). The results show that for the 1 nm width ultra-thin layer, which is 40 times thinner than the ultra-thin film and we call nano-wire, a big gap is created in the maximum amount for LAEF compared with other widths. This can be the result of less plasmonic resonance efficiency. On the other hand, as shown in Figure 12(b), the LAEF curves show yet much better absorption than bare-slit MSM-PDs which indicate the nano-wire acts as an active waveguide to support propagating modes created from plasmonic interactions.

Hence, due to creation of an improved coupling medium for SPP modes and localized plasmatic regions inside the active region of thin-film assisted EW MSM-PDs, an efficient light concentration is achieved for the substrate which results in quality light absorption and high values of LAEF in corresponding absorption curves compare with bare slit and nano-wire assisted plasmonics-based MSM-PDs.

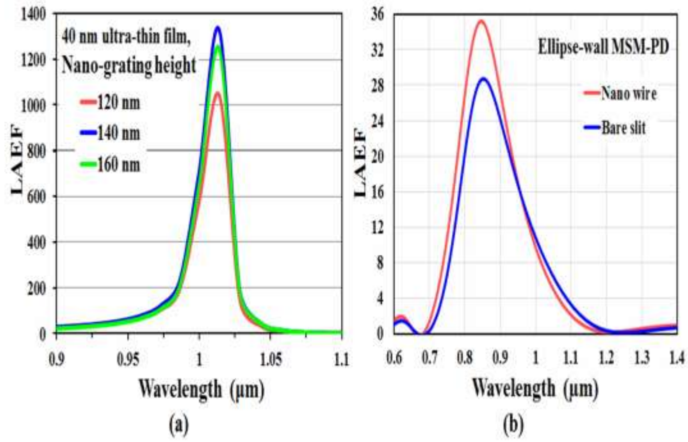

Figure 12. Light absorption enhancement curves for plasmonics MSM-PDs utilizing ellipse-wall nano-grating. (a) 40 nm width thin film layer with outstanding optical properties applied inside the central slit of MSM-PDs with different nano-grating heights, (b) Two different designs with simple central slit and a thin nano-wire assisted-slit, which only covers 1 nm of the slit surface, are compared (Masouleh *et al.*, 2015).

Figure 13 shows different number of nano-gratings (i.e., N = 1 ~ 9) applied on both sides of the slit in ultra-thin film assisted MSM-PD with the nano-grating thickness of 140 nm. It is interesting to observe that the LAEF curves behavior for the ultra-thin film assisted MSM-PD is changing while the number of nano-gratings is the same like the plasmonics-based MSM-PD without thin film as presented in Figure 13.

There has been considerable interest in modelling and simulation of plasmonic devices such as, plasmonic MSM-PDs mostly on geometrical subwavelength features i.e., peripheral gratings, double gratings, and kinds of nano-particle assisted plasmonic MSM-PDs, furthermore optimization of nano-gratings cross-section is always a useful variable to study in plasmonic related researches. Most techniques lie within carefully matching the wavelength of the illumination light with the dimension of plasmonic components and careful meshing designs to get reliable results. Although previous researches are considered to be valuable data and the basics for development of MSM-PDs, they didn't report an outstanding improvement in functionality of the MSM-PDs.

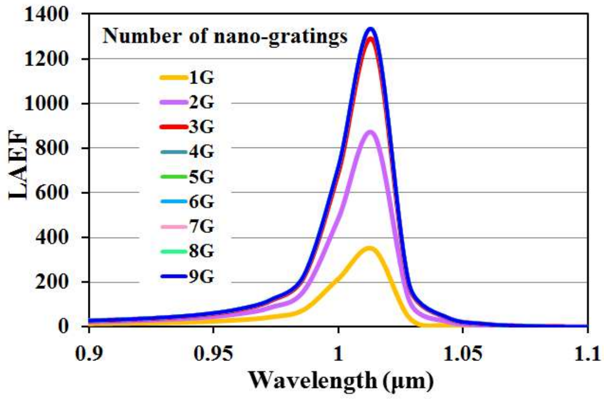

Figure 13. LAEF spectra for ellipse-wall MSM-PDs with different nano-grating numbers (i.e., N = 1 ~ 9) on each side of the slit. The nano-grating's height is 140 nm (Masouleh *et al.*, 2015).

Meanwhile, we developed an ultra-thin film assisted device with a substantially high light absorption capacity in contrast with the existing plasmonic MSM-PDs as reported. The control of light stimulation with surface plasmon effects in subwavelength scale is among one of the popular variables in nano-photonic circuits studies. The results would assist in the development of plasmonics-based photodetectors.

8.5. Field distribution in various plasmonic-based MSM-PD devices.

For MSM-PDs with the same slit widths, the LAEF is considerably improved if the ultra-thin film is placed symmetrically in the sub-wavelength apertures. We have evaluated the influence of metallic thin films for the light absorption performance of various MSM-PDs through the modeling and simulation.

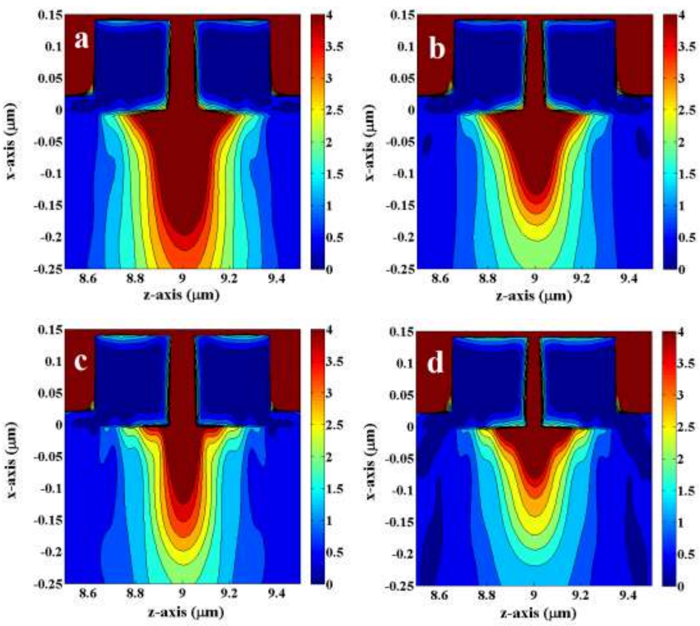

Figure 14. Electric field intensity distribution in the cross-section overview for plasmonic-based MSM-PD with rectangular-shaped nano-grating on the substrate. The conditions are: (a) 100 nm slit width, (b) 50 nm slit width, also for plasmonic-based MSM-PD with thin film layer, (c) 5 nm height and 90 nm width for 100 nm sub-wavelength slit, and (d) 5 nm height and 40 nm width for 50 nm sub-wavelength slit. The duty cycle, underlayer thickness, and nano-grating thickness of the device are 40%, 20 nm, and 120 nm, respectively.

To obtain a better insight in light absorption properties due to this special geometry, the electric field distribution in the cross section of the simple plasmonic-based MSM-PDs with 50 nm and 100 nm sub-wavelength slit width, plasmonic-based MSM-PD with 5-nm height and 40 nm width thin film when the slit width is 50 nm, and also plasmonic-based MSM-PD with 5-nm height and 90 nm width thin film when the slit width is 100 nm are shown in Figure 14, as the summation of the electric field components intensity distribution in the area.

The Electric field density plots confirm that thin film-assisted devices are much efficient in power localization compared with the plasmonic-based MSM-PD without a thin film in the slit. Also, we expected for 50 nm slit width, the components of the electric filed are well-focused because it has higher LAEF.

As expected, the plasmonic lens character which is involved with energy localization using nano-sized features is provided once an ultra-thin metallic film with improved optical characteristics is applied inside the active region, hence enhances the SPP resonances and light absorption inside the device active region.

8.6. Modeling Structures Close to the Reality.

To obtain more accurate model that is suitable for experimental purposes, we have to take into account every effective factor which might have an influence on the device behavior or characteristics. The results reported on the shape of nano-structures cross section have confirmed that no matter how much efforts put to build similar and defect less structure, one will end up having the nano-structures which are slightly different in shape compared to each other. Hence, we have decided to design the MSM-PDs which have a combination of different nano-grating shapes.

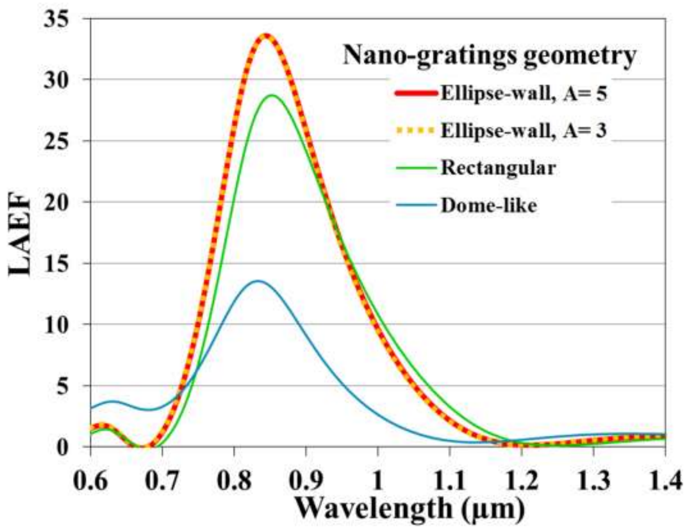

Figure 15. LAEF spectrum of ellipse-wall nano-gratings with exponential coefficients of 3 and 5, rectangular, and dome-like shaped nano-gratings.

Figure 15 shows the curvature change of the ellipse-wall nano-gratings, where A=3 or 5 have no substantial effect on the LAEF, while as we expected, the maximum LAEF belongs to the ellipse-wall design compared with the other two shapes. Randomly arranging these four different nano-grating geometries, we will have a non-uniform nano-grating MSM-PD. The results for this non-uniform design, using the mixed arrangement of the shapes is shown in Figure 15 and Figure 16. It is obvious that mixing ellipse-wall nano-gratings of different exponential coefficients (A) with any order provides almost the same absorption curve.

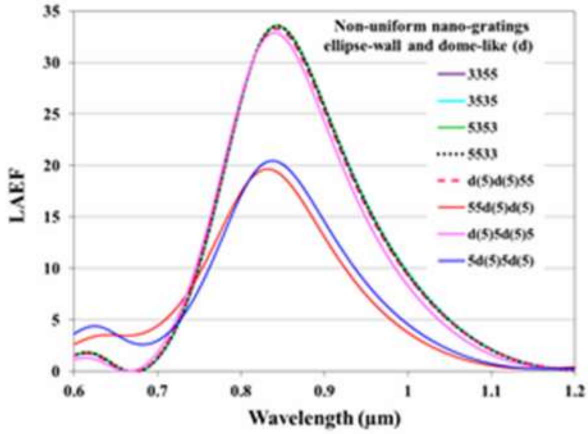

Figure 16. Non-uniform design of ellipse-wall nano-gratings, and dome-like nano-gratings, d, both with exponential coefficients of 3 and 5.

However, the simulations show that the combination of dome-like and ellipse-wall nano-gratings with A=5, while the dome-like structure is the closest grating to the slit, will change the LAEF significantly

This brings us the opportunity to examine a device's behavior which has some flaw in the nano-structure's manufacturing process.

Here, we have presented simulation results for rectangular, dome-like and ellipse-wall shaped nano-gratings, which are the most probable geometries one might end up with experimentally. The dome-like shape is similar to a triangular shaped cross-section nano-grating but with curved walls as in EW nano-gratings.

9. CONCLUSIONS

Increasing efforts have been made to develop nanoscale metallic light interaction, simply plasmonics. Development of ultra-small optoelectronic devices with plasmonic elements offer the ability to manipulate light in nano-scale volumes while the devices are optimized towards having high-speed performance and broader bandwidth. These properties with aim of producing smaller optical and photonic circuits has also made an impression on nanoscale device development such as, photodetectors for commercial and industrial use. The simulated results reveal that symmetrically and periodically designed plasmonic MSM-PD devices integrated with plasmonic features provide a substantial light absorption enhancement. The main approaches involving in MSM-PD improved function are ultra-thin film design in the central slit which further enhances light capturing and provides extra-focus, also the metallic nano-grating which are responsible for wave vector mixing process and leading the light through the structure and making a focal point in the central slit, and last but not least the Fabry-Perot resonances inside the central slit. Hence, nano-sized MSM photodetectors, involving plasmonics, acquired high-responsivity and low-loss characteristics making them able to recover the electromagnetic energy which would have been lost without this technology, therefore made them more reliable for wireless network systems and high-speed optical communication technology. Surface plasmon resonances have found practical applications in sensitive nanoscale photodetectors. For instance, the TM-polarized light is suitable for excitation of surface plasmon resonances through subwavelength slits in metallic films flanked by metallic nano-gratings in plasmonics-based MSM-PDs. In this review, a couple of different nano-grating assisted MSM-PDs were designed, and their performance under light illumination was studied. Parameters such as, light absorption enhancement, light reflection factor, and total field distribution were introduced to study different metallic nano-structures impression such as, varied cross-section shapes or grooves, on the device behavior. In addition, the concept of SPPs excited at metal-dielectric interface has been introduced which are suitable for plasmonics-based applications. The light absorption as a result of light interaction with the subwavelength slit, metal nano-gratings, and ultra-thin film inside the slit were also discussed which well proves the extraordinary optical absorption involved with these phenomena.

Using FDTD algorithm and defining characteristics of involved materials with Drude-Lorentz dielectric function provide promising condition to maximize the device's functionality and improve the energy flow (i.e., light intensity) into the detector's active region. Furthermore, the light capturing efficiency of MSM-PD devices is highly dependent on the impact of nano-structure's geometry and design. FDTD method is an advantageous technique with the ability to analyze arbitrary shapes and can easily study the impact of the optimized physical and geometrical parameters on the amount of transmitted light into the MSM-PD structure. Hence, using this method, the performance of nano-grating assisted MSM-PDs with different geometrical parameters such as, subwavelength slit width, nano-grating heights, inside the slit design and other structural parameters (e.g., corrugation shapes) for maximized light absorption enhancement were easily calculated.

The resonant coupling of incident light wave with the nano-gratings wave vector leads to SPPs excitation and energy transmission in the next step. This is caused by increased effective impedance resulting from corrugation design on the surface. The main impetus for considering such nano-gratings design on MSM-PD's metallic contacts is the opportunity to assist and improve the light transmission in nano-scale, e.g., central slit. Making a comparison between the plasmonic MSM-PD with conventional MSM-PD confirms creation of plasmonic lens in the former design because of the energy localized region and focal point at nanoscale. Furthermore, applying nano-structured features on the metallic electrodes and the opportunity to shrink the area between the electrodes, namely the central slit, improves the optical response of the device. These useful characteristics further improve, once the ultra-thin layer is added inside the slit.

These simulation results have shown that the nano-structured MSM-PDs can theoretically attain a maximum light absorption of almost 35-times near the design wavelength (for ellipse-wall nano-grating assisted MSM-PD), and a better performance is achieved implementing an ultra-thin film in the MSM-PD design, which results in more than a 1000 times energy absorption. However, some values in between would be more realistic for light enhancement in the practical devices.

This review's aim was to show the optimized behavior of MSM-PD while the geometrical parameters are changed. The results suggest that some parameters optimization are more influential than others. These results provide useful information for the design and fabrication of nanoscale optoelectronic devices. Several samples of nano-structured MSM-PDs can be manufactured using the FIB lithography based on the characterized nano-grating groove profiles obtained as optimized according to this study. The presented results assists in improving the concept of novel high responsivity, plasmonics-based MSM-PDs for high speed applications and easy implementation in optical communication and network systems, such as, urban lighting, security, robots, military, biomedical sensing and many others.

5. REFERENCES

Agrawal, G.P. **(2002)**. Fiber-Optic Communication Systems. *John Wiley & Sons*, Inc., Fourth Edition.

Akarca-Biyikli, S., Bulu, I., Ozbay, E. **(2004)**.Enhanced transmission of microwave radiation in one-dimensional metallic gratings with subwavelength aperture. *Appl. Phys. Lett.* 85, 1098-1100.

Atwater, H.A. **(2007)**. The promise of plasmonics. *Scientific American*, 296, 4, 56-62.

Battula, A., Lu, Y., Knize, R.J., Reinhardt, K., Chen, S. **(2007)**. Extraordinary transmission and enhanced emission with metallic gratings having converging-diverging channels. *Act. Passive Electron. Compon.*

Bera M., Ray, M. **(2012**). Role of waveguide resonance in coupled plasmonic structures using bimetallic nanofilms. *Opt. Eng.* 51, 103801.

Beruete, M., *et al.* (2004). "nhanced millimeter-wave transmission through subwavelength hole arrays. Opt. Lett. 29, pp. 2500-2502.

Bozhevolnyi, S.I., Volkov, V.S., Devaux, E., Ebbesen, T.W. **(2005)**. Channel plasmon-polariton guiding by subwavelength metal grooves. *Phys. Rev. Lett*. 95, 1-4.

Ceglia, D., Vincenti, M.A., Scalora, M., Akozbek, N., Bloemer, M.J. *(2010)*. Enhancement and inhibition of transmission from metal gratings. *Engineering the Spectral Response, arXiv:1006.3841, 1-25.*

Chong, C., Kumar, S.P. **(2003)**. Sensor networks: evolution, opportunities, and challenges. *Proceedings of the IEEE* 91, 8, 1247-1256.

Collin, S., Pardo, F., Teissier, R., Pelouard, J.L. **(2002)**. Horizontal and vertical surface resonances in transmission metallic gratings. *Journal of Optics A: Pure and Applied Optics* 4, 154-160.

Darrin, M.A.G., Carkhuff, B.G., Mehoke, T.S. **(2004)**. Future Trends in Miniaturization for Wireless Applications. *Johns Hopkins APL Technical Digest* 25, 4, 343-347.

Das, N., Masouleh, F.F., Mashayekhi, H.R. **(2014)**. Light Absorption and Reflection in Nanostructured GaAs Metal-Semiconductor-Metal Photodetectors. *IEEE Transactions on Nanotechnology*, 13, 5, 982-989.

Das, N.K., Tan, C.L., Lysak, V.V., Alameh, K., Lee, Y.T. **(2009)**. Light absorption enhancement in metal-semiconductor-metal photodetectors using plasmonic nanostructure gratings, *6th International Symposium on 'High capacity Optical Networks and Enabling Technologies' HONET'09*, Alexandria, Egypt. 86-90.

Das, N.K., Karar, A., Vasiliev, M., Tan, C.L., Alameh, K., Lee, Y.T. **(2010)**. Groove shape dependent absorption enhancement of 850 nm MSM photodetectors with nano-gratings. *Proceedings of the 10th Int'l. Conf. on Nanotechnology 'IEEE NANO 2010'*, Seoul, South Korea.

Das, N.K., Karar, A., Vasiliev, M., Tan, C.L., Alameh K., Lee, Y.T. **(2011)**. Analysis of nano-grating-assisted light absorption enhancement in metal–semiconductor–metal photodetectors patterned using focused ion-beam lithography. *Opt. Commun.* 284, 1694-1700.

Das, N., Islam, S. **(2012)**. Optimization of nano-grating structure to reduce the reflection losses in gaas solar cells. 22nd Australasian Universities Power Engineering Conference 2012 (AUPEC2012), 1-5, Sept. 26-29. *University of Tasmania, Hobart, Australia*.

Dhakal, D. **(2009)**. Analysis of the sub-wavelength grating in OptiFDTD simulator. *M.Sc. Thesis, School of Eng. and Science*, Jacobs Univ., Bremen, Germany, Ch. 1.

Finite Difference Time Domain Photonics Simulation Software. *OptiFDTD Technical background and Tutorials*, Version 8.

Grote, R., Osgood, R.M., Spanier, J.E., Nabet, B. **(2010)**. Optimization of a surface plasmon enhanced metal-semiconductor-metal photo detectoron Gallium Arsenide. *Proc. Frontiers in Optics, OSA Technical Digest (CD) (Optical Society of America)*, paper FThY3.

Hibbins, A.P., Evans, B.R., Sambles, J.R. **(2004)**. Experimental Verification of Designer Surface Plasmons. *Science* 308, 670-672.

Ian-Akyildiz, et. al. **(2002)**. Wireless sensor networks: a survey. *Computer networks* 38, 4, 393-422.

Jin, J.M. **(2010)**. Theory and Computation of Electromagnetic Fields. *John Wiley & Sons*.

Karar, A., Das, N., Tan, C.L., Alameh, K., Lee, Y.T., Karouta, F. **(2011)**. High-responsivity plasmonics-based GaAs metal-semiconductor-metal photodetectors. *Appl. Phys. Lett.* 99, 133112, 1-3.

Kim, S., Lim, Y., Kim, H., Park, J., Lee, B. **(2008)**. Optical beam focusing by a single subwavelength metal slit surrounded by chirped dielectric surface gratings. *Appl. Phys. Lett.*, 92, 1-3.

Kikuta, H., Toyota, H., Yu, W.J. **(2003)**. Optical elements with subwavelength structured surfaces. *Optical Review* 10, 2, 63-73.

Ko, D.H. *et al.* **(2011)**. Light-trapping nano-structures in organic photovoltaic cells. *Journal of Materials Chemistry* 21, 41, 16293-16303.

Krenn, J.R., Salerno, M.N.F., Lamprecht, B., Schider, G., Leitner, A., Aussenegg, F.R., Weeber, J.C., Dereux, A., Goudonnet, J.P. **(2001)**. Light field propagation by metal micro- and nanostructures. *Journal of Microscopy* 202, 122-128.

Lee, K.L., Lee, C.W., Wei, P.K. **(2007)**. Sensitive detection of nanoparticles using metallic nanoslit arrays. *Appl. Phys. Lett.*, 90, 1-3.

Lezec, H.J., Degiron, A., Devaux, E., Linke, R.A., Martin-Moreno, L., Garcia-Vidal, F.J., Ebbesen, T.W. **(2002)**. Beaming Light from a Subwavelength slit. *Science* 297, 5582, 820-822.

Lindquist, N.C., Nagpal, P.K., McPeak, M., Norris, D.J., Oh, S. **(2012)**. Engineering metallic nanostructures for plasmonics and nanophotonics. IOP Publishing Ltd, *Reports on Progress in Physics* 75, 3.

Liu, Z., Durant, S., Lee, H., Pikus, Y., Fang, N., Xiong, Y., Sun, C., Zhang, X. **(2007)**. Far-Field Optical Superlens. *Nano Lett.*, 7, 2, 403-408.

Makki, K.S., Reiher, P., Makki, K., Pissinou, N., Makki, S. **(2007)**. Mobile and Wireless Network Security and Privacy. *Springer Science & Business Media*.

Markovic, M.I., Rakic, A.D. **(1990)**. Determination of reflection coefficients of laser light of wavelength from the surface of aluminum using the Lorentz-Drude model. *Appl. Opt.* 29, 3479-3483.

Martín-Moreno, L., García-Vidal, F.J., Lezec, H.J., Pellerin, K.M., Thio, T., Pendry, J.B., Ebbesen, T.W. **(2001)**. Theory of extraordinary optical transmission through subwavelength hole arrays. *Phys. Rev. Lett.* 86, 1114-1117.

Martín-Moreno, L., García-Vidal, F.J., Lezec, H.J., Degiron, A., Ebbesen, T.W. **(2003)**. Theory of highly directional emission from a single subwavelength aperture surrounded by surface corrugations. *Physical Review Letters*, 90.

Masouleh, F.F., Das, N.K., Mashayekhi, H.R. **(2013)**. Comparison of different plasmonic nano-grating profiles for quality light absorption in nano-structured MSM photo-detectors. *Opt. Eng.*, 52, 12, 127101.

Masouleh, F.F., Das, N.K., Mashayekhi, H.R. **(2014)**. Assessment of amplifying effects of ridges spacing and height on nano-structured MSM photo-detectors. *Journal of Optical and Quantum Electronics* 46, 4.

Masouleh, F.F., Das, N.K., Mashayekhi, H.R. **(2013)**. Optimization of light transmission efficiency for nano-grating assisted MSM-PDs by varying physical parameters. *Phot. Nano. Fund. Appl.*, 12, 1, 45-53.

Masouleh, F.F., Das, N., Rozati, S.M. **(2015)**. Optimal subwavelength design for efficient light trapping in central slit of plasmonics-based metal-semiconductor-metal photodetector. *Optical and Quantum Electronics* 47, issue 6, 1477-1485.

Mawet, D., Riaud, P., Baudrand, J., Boccaletti, A., Baudoz, P., Rouan, D., Lenaerts, C., Surdej, J. **(2006)**. Achromatic optical vortex coronagraph with subwavelength gratings. *Proceedings of the Int. Coronagraph Workshop*, Pasadena, CA, USA, 69-72.

Noor, Z., Ragab, K., Abdullah, A.B. **(2012)**. Wireless Sensor Networks and Energy Efficiency: Protocols, Routing and Management. *IGI Global*.

Ozbay, E. **(2006)**. Plasmonics: Merging Photonics and Electronics at Nanoscale Dimensions. *Science* 311, 5758, 189-93.

Pal, B.P. **(1992)**. Fundamentals of Fibre Optics in Telecommunication and Sensor Systems. *Bohem press*.

Park, W. **(2014)**. Optical interactions in plasmonic nanostructures. *Nano Convergence,* 1, 2, 1-27.

Pendry, J.B. **(2000)**. Negative Refraction Makes a Perfect Lens. *Phys. Rev. Lett.* 85. 3966-3969.

Porto, J.A., García-Vidal, F.J., Pendry, J.B**. (1999)**. Transmission resonances on metallic gratings with very narrow slits. *Physical Review Letters* 83, 2845-2848.

Porto, J.A., García-Vidal, F.J., Pendry, J.B**. (1999)**. Transmission resonances on metallic gratings with very narrow slits. *Physical Review Letters* 83, 2845-2848.

Raether, H. **(1988)**. Surface Plasmons on Smooth and Rough Surfaces and on Gratings. *Springer-Verlag*, Berlin.

Rakic, A.D., Djurišic, A.B., Elazar, J.M., Majewski, M.L. **(1998)**. Optical Properties of Metallic Films for Vertical-Cavity Optoelectronic Devices. *Applied Optics,* 37, 22, 5271-5283.

Sambles, J.R., Bradbery, G.W., Yang, F. **(1991)**. Optical excitation of surface plasmons: an introduction. *Contemporary physics* 32, 3, 173-183.

Schmid, J.H., Cheben, P., Janz, S., Lapointe, J., Post, E., Delage, A., Densmore, A., Lamontagne, B., Waldron, P., Xu, D.X. **(2008)**. Subwavelength Grating Structures in Silicon-on-Insulator Waveguides. Hindawi Publishing Corporation, *Advances in Optical Technologies*, *685489, 1-8.*

Shackleford, J.A., Grote, R., Currie, M., Spanier, J.E., Nabet, B. **(2009)**. Integrated plasmonic lens photodetector. *Appl. Phys. Lett.* 94.

Shalaev, V.M. **(2007)**. Optical negative-index metamaterials. *Nature Photonics* 1, 41-48.

Sharma, A.K., Zaidi, S.H., Logofătu, P.C., Brueck, S.R.J. **(2002)**. Optical and Electrical Properties of Nanostructured Metal-Silicon-Metal Photodetectors. *IEEE J. Quantum Electron*. 28, 12,1651–1660.

Shen, H., Bienstman, P., Maes, B. **(2009)**. Plasmonic absorption enhancement in organic solar cells with thin active layers. *J. Appl. Phys.* 106, 073109.

Sturman, B., Podivilov, E., Gorkunov, M. **(2008)**. Theory of extraordinary light transmission through arrays of subwavelength slits. *Phys. Rev. B* 77, 075106.

Tan, C.L., Lysak, V.V., Alameh, K., Lee, Y.T. **(2010)**. Absorption enhancement of 980 nm MSM photodetector with a plasmonic grating structure. *Opt. Commun.* 283, 1763-1767.

Veselago, V.G. **(1968)**. The electrodynamics of substances with simultaneous negative values of ε and μ. *Physics-Uspekhi* 10, 4, 509-514.

White, J.S., Veronis, G., Yu, Z., Barnard, E.S., Chandran, A., Fan, S., Brongersma, M.L. (2006). Extraordinary optical absorption through subwavelength slits. *Opt. Lett.* 34, 686-688.

Wijesinghe, T., Premaratne, M. **(2012)**. Dispersion relation for surface plasmon polaritons on a Schottky junction. *Optics Express* 20, 7151-7164.

Yee, K.S. **(1966)**. Numerical solution of initial boundary value problems involving maxwell's equations in isotropic media. *IEEE Transactions on Antennas and Propagation* 14, 3, 302-307.

Yoon, K.H., Shuler, M.L., Kim, S.J. **(2006)**. Design optimization of nano-grating surface plasmon resonance sensors. *Opt. Express*, 14, 4842-4849.

Yu, Z., Veronis, G., Fan, S., Brongersma, M.L. **(2006)**. Design of midinfrared photodetectors enhanced by surface plasmons on grating structures. *Appl. Phys. Lett.* 89, 151116.

Yu, W. **(2009)**. Electromagnetic Simulation Techniques Based on the FDTD Method. *John Wiley & Sons*.

Zalevsky, Z., Abdulhalim, I. **(2010)**. Integrated *Nanophotonic Devices* 6, William Andrew.

Zhang, X., Liu, Z. **(2008)**. Superlenses to overcome the diffraction limit. *Nat. Mater.* 7, 435-441.

Zhang, W., Azad, A.K., Han, J. **(2007)**. Resonant Excitation of Terahertz Surface Plasmons in Subwavelength Metal Holes. *Hindawi Publishing Corporation*, Active and Passive Electronic Components.

Zimmermann, H. **(2004)**. Silicon Optoelectronic Integrated Circuits. *Springer Berlin Heidelberg* 13, 1-23.

6. CONFLICTS OF INTEREST

The authors declare no conflict of interest.